Liquid-phase-epitaxy-grown $InAs_xSb_{1-x}$/GaAs for room-temperature 8–12 μm infrared detectors

Changtao Peng,[a] NuoFu Chen,[b] Fubao Gao, Xingwang Zhang, Chenlong Chen, Jinliang Wu,[b] and Yude Yu
Key Laboratory of Semiconductor Materials Science, Institute of Semiconductors, Chinese Academy of Sciences, P.O. Box 912, Beijing 100083, China

(Received 30 November 2005; accepted 21 April 2006; published online 13 June 2006)

High-quality $InAs_xSb_{1-x}$ ($0<x\leqslant 0.3$) films are grown on GaAs substrates by liquid phase epitaxy and electrical and optical properties of the films are investigated, revealing that the films exhibit Hall mobilities higher than 2×10^4 cm^2 V^{-1} s^{-1} and cutoff wavelengths longer than 10 μm at room temperature (RT). Photoconductors are fabricated from the films, and notable photoresponses beyond 8 μm are observed at RT. In particular, for an $InAs_{0.3}Sb_{0.7}$ film, a photoresponse of up to 13 μm with a maximum responsivity of 0.26 V/W is obtained at RT. Hence, the $InAs_xSb_{1-x}$ films demonstrate attractive properties suitable for room-temperature, long-wavelength infrared detectors. © *2006 American Institute of Physics*. [DOI: 10.1063/1.2209709]

Long-wavelength (8–12 μm) infrared detectors that can operate at room temperature (RT) have important infrared applications. At present, $Hg_{1-x}Cd_xTe$ is the most prevalent material in high-performance, long-wavelength infrared detectors. However, $Hg_{1-x}Cd_xTe$ lacks stability and uniformity over a large area, and only works under cryogenic conditions. $InAs_xSb_{1-x}$ has recently attracted interest as a promising alternative to $Hg_{1-x}Cd_xTe$. $InAs_xSb_{1-x}$ is more stable and has higher electron and hole mobilities than $Hg_{1-x}Cd_xTe$. When the value of x is in the midrange ($0.2<x<0.6$), $InAs_xSb_{1-x}$ exhibits a large, positive "optical bowing" effect due to the ordering in the alloy,[1–4] making possible its application in long-wavelength infrared detection. The main disadvantage of $InAs_xSb_{1-x}$ is a lack of lattice-matched substrates. Despite its large lattice mismatch ($7.2\% < \Delta a/a < 14.6\%$) with $InAs_xSb_{1-x}$, GaAs is an excellent substrate because of its infrared transparency and low noise. Moreover, it helps integrate detection and signal processing circuits and reduce parasitic capacitances.[5] Therefore, the crucial point is the growth of high-quality $InAs_xSb_{1-x}$ films on GaAs substrates ($InAs_xSb_{1-x}$/GaAs). Epitaxial $InAs_xSb_{1-x}$ films have been grown on GaAs substrates by molecular beam epitaxy[5–9] (MBE) and metal organic chemical vapor deposition (MOCVD).[10–14] Furthermore, demonstrations of RT long-wavelength infrared photodiodes[13] and photoconductors[14] using the MOCVD-grown $InAs_xSb_{1-x}$/GaAs have been reported.

As is much more accessible and economical than MBE and MOCVD, liquid phase epitaxy (LPE) is often considered for the growth of $InAs_xSb_{1-x}$ films. However, it is difficult to use LPE to carry out epitaxial growth with a large lattice mismatch ($\Delta a/a>1\%$). Popov *et al.*[15] have grown $InAs_xSb_{1-x}$ films on InAs substrates, indicating that when $x<0.7$ the $InAs_xSb_{1-x}$ films grown were polycrystalline ($\Delta a/a>2.1\%$). Recently, Dixit *et al.*[16] have reported successful epitaxial growth of $InAs_xSb_{1-x}$/GaAs by LPE with extremely low ramp-cooling rates (<0.8 °C/h), but they could incorporate only 6 at. % arsenic in $InAs_xSb_{1-x}$ films due to the miscibility gap. This obstructs their $InAs_xSb_{1-x}$/GaAs from being applied above the 9.5 μm wavelength range. In this letter, we report high-quality LPE-grown $InAs_xSb_{1-x}$/GaAs suitable for RT long-wavelength infrared detectors.

The LPE growth was carried out in a conventional horizontal graphite sliding-boat system with an ambient of flowing Pd-membrane purified hydrogen at atmospheric pressure in a quartz reactor tube. The starting materials were 6*N* pure In and Sb, and undoped InAs ($n<10^{17}$ cm^{-3}). The substrates used were well-polished, semi-insulating (100) GaAs wafers. In this work, samples were grown at constant growth temperatures rather than in ramp-cooling routines. Constant growth temperatures help the uniformity of the $InAs_xSb_{1-x}$ films in the growth direction. The growth temperatures (T_G) for the samples are shown in Table I. The thicknesses of the $InAs_xSb_{1-x}$ films range from 10 to 20 μm.

The inset of Fig. 1 shows a cross section image of a typical sample (C) observed under a scanning electron microscope (SEM), indicating a sharp interface between the $InAs_xSb_{1-x}$ film and GaAs substrate. The energy dispersive x-ray analysis (EDAX) system of the SEM was used for compositional analysis of the $InAs_xSb_{1-x}$ films. By linescan of EDAX perpendicular to the surface in the cross section, the distribution of the constituent elements along the depth direction can be obtained. The EDAX linescan result of sample C is shown in Fig. 1, indicating the composition uni-

TABLE I. Growth temperatures (T_G), compositions (x) obtained from EDAX and XRD, results of the Hall measurements at RT, and band gaps (E_g) obtained from the FTIR data for the $InAs_xSb_{1-x}$ films. $E_{g,w}$ denotes band gaps at 300 K calculated from the equation of Woolley and Warner.

Sample	T_G (°C)	x EDAX	x XRD	Hall mobilities (cm^2 V^{-1} s^{-1})	Carrier concentration n type (cm^{-3})	E_g (eV)	$E_{g,w}$ (eV)
A	432	0.11	0.10	2.62×10^4	1.09×10^{17}	0.131	0.139
B	545	0.25	0.24	2.26×10^4	2.56×10^{17}	0.122	0.108
C	549	0.30	0.30	2.03×10^4	2.92×10^{17}	0.118	0.102

[a]Electronic mail: ctpeng@red.semi.ac.cn
[b]Also at National Microgravity Laboratory, Institute of Mechanics, Chinese Academy of Sciences, Beijing 100080, China.

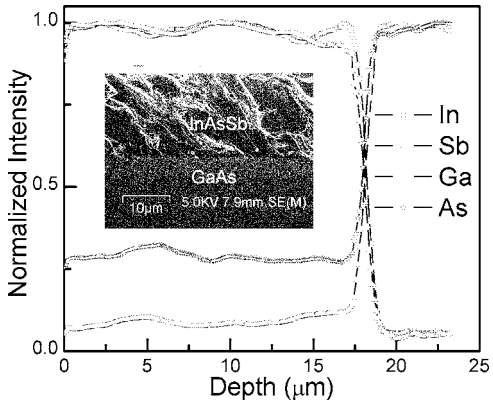

FIG. 1. Distribution of the constituent elements along the depth direction obtained from EDAX linescan for sample C. Inset shows a cross section SEM image of sample C.

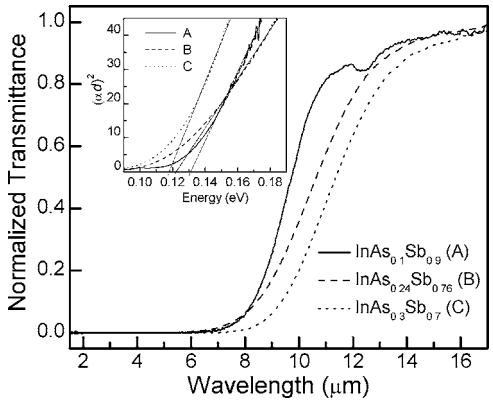

FIG. 3. Fourier transform infrared transmission spectra at room temperature of the $InAs_xSb_{1-x}$ films. Inset shows the corresponding $(\alpha d)^2$ for linear fitting.

formity of the $InAs_xSb_{1-x}$ film and confirming the sharpness of the interface. Hence, in our LPE growth, severe diffusion at the interface did not occur even for sample C with a high growth temperature of up to 549 °C, and $InAs_xSb_{1-x}$ films with uniform composition can be grown by applying constant growth temperatures. The compositions (x) of the samples obtained from EDAX are shown in Table I.

Figure 2 shows a typical x-ray diffraction (XRD) pattern of the samples, indicating that the $InAs_xSb_{1-x}$ films are polycrystalline with (100)-preferred orientation. For comparison, the inset shows the predominant (400) reflection peaks from the three samples and an InSb film. The (400) peaks obviously shift towards higher angle with the increase of arsenic mole fraction (x). According to Vegard's law, the compositions of the $InAs_xSb_{1-x}$ films can also be calculated from those XRD peaks and the results, shown in Table I, are consistent with those obtained from EDAX, considering that the accuracy of EDAX, is within ±1 at. %.

The polycrystalline structure of the $InAs_xSb_{1-x}$ films confirms that, as mentioned above, it is quite difficult to grow epitaxial $InAs_xSb_{1-x}$/GaAs by LPE. In general, epitaxial structures are preferred over polycrystalline structures because grain boundaries that exist in polycrystalline structures degrade the material quality. For instance, scattering from grain boundaries greatly lowers mobility. However, the results of Hall measurements at RT, shown in Table I, reveal that the $InAs_xSb_{1-x}$ films have high Hall mobilities greater than 2×10^4 cm^2 V^{-1} s^{-1} at RT, which are at the same level as those reported for epitaxial $InAs_xSb_{1-x}$/GaAs with similar composition grown by MOCVD (Ref. 12) and MBE.[6,8] This may be explained as follows. A lot of misfit dislocations exist in the epitaxial $InAs_xSb_{1-x}$/GaAs grown by MOCVD and MBE due to the large lattice mismatch, and dislocation scattering has been regarded as one of the dominant scattering mechanisms for $InAs_xSb_{1-x}$/GaAs.[12,17] However, for our $InAs_xSb_{1-x}$ films, the inside-grain dislocation density could be greatly reduced due to the nearly equilibrium growth conditions in LPE. Moreover, the highly (100)-preferred orientation would diminish the effect of grain boundaries. Hence, it may be counteracted by the reduction of the inside-grain dislocation density.

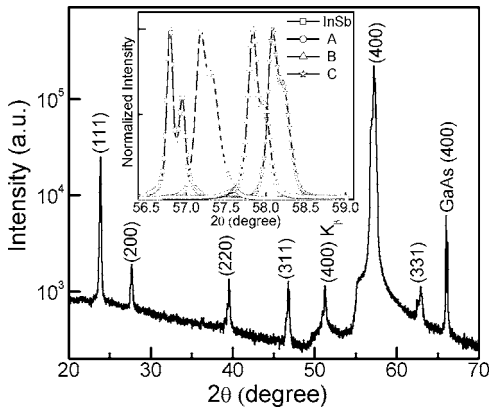

FIG. 2. Typical x-ray diffraction pattern of the samples. Inset shows the predominant (400) reflection from an InSb film and the samples.

The Fourier transform infrared (FTIR) transmission spectra of the samples were measured at RT, and using that of a GaAs substrate as reference, the FTIR transmission spectra of the corresponding $InAs_xSb_{1-x}$ films at RT were obtained and are shown in Fig. 3. The absorption edges of the $InAs_xSb_{1-x}$ films shift toward the long-wavelength side with the increase of x, demonstrating a strong positive optical bowing effect. For a direct energy gap semiconductor, the absorption coefficient (α) of $InAs_xSb_{1-x}$ can be described as $\alpha=A\ (h\nu-E_g)^{1/2}$. Here A is a constant, ν is the incident photon frequency, and E_g is the band gap. Therefore, based on the data of αd (d is the film thickness) calculated from the FTIR transmission results, E_g at RT can be obtained from the linear fitting of $(\alpha d)^2$ (as shown in the inset of Fig. 3) and is shown in Table I. The dependence of E_g on the composition of $InAs_xSb_{1-x}$ at RT has been given by Woolley and Warner[18] as $E_g(x)=0.35-0.771(1-x)+0.596(1-x)^2$ eV. The E_g calculated from this equation ($E_{g,w}$), also shown in Table I, does not agree with our results. The E_g of $InAs_xSb_{1-x}$ may be influenced by the degree of ordering[1] and residual strain[19] in the alloy, so the discrepancy may be attributed to the difference between growth processes in producing ordering and residual strain.

Photoconductors formed by 0.1×2 mm^2 bars of $InAs_xSb_{1-x}$ films were fabricated on samples A and C. Au/Ti was used to form an Ohmic contact. The spectral photoresponse was measured at 77 K and RT using a FTIR spectrometer, and the absolute responsivity was calibrated based on the responsivity measurement at 77 K using a standard blackbody source with a temperature of 800 K. The bias voltage applied to the photoconductors was 1.5 V. Figures 4(a) and 4(b) show the spectral responsivities of the photo-

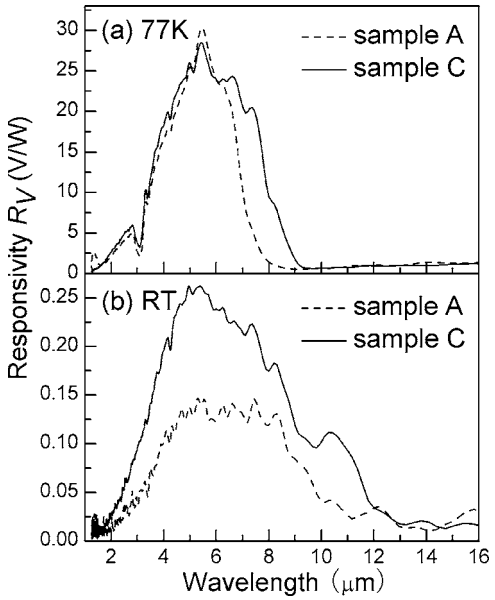

FIG. 4. Spectral responsivity of the photoconductors fabricated on samples A and C at (a) 77 K and (b) room temperature.

conductors at 77 K and RT, respectively. A notable photoresponse beyond 8 μm was observed with both photoconductors at RT, and the cutoff wavelength was extended to about 13 μm. The maximum responsivities ($R_{v,\max}$) and the cutoff photon energies (E_c) of the photoconductors are shown in Table II. At RT the responsivities of our photoconductors are higher than those reported for MOCVD-grown $InAs_xSb_{1-x}/GaAs$.[13,14] This confirms the high quality of our LPE-grown $InAs_xSb_{1-x}/GaAs$. In particular, sample C with a midrange composition exhibited a discernible photoresponse of up to 13 μm with a maximum responsivity of 0.26 V/W at RT, showing great potential for RT long-wavelength infrared detection.

In comparison with the E_g obtained from the FTIR experiments, E_c is smaller by about 0.02 eV for both samples. The temperature dependence of E_g is described by Varshni's equation:[20] $E_g(T)=E_g(0)-\alpha T^2/(\beta+T)$. Using the values of α and β for $InAs_xSb_{1-x}$ fitted by Dixit *et al.*,[16] $\alpha=3.01\times10^{-4}$ eV K^{-1} and $\beta=341$ K, the difference between the E_g at 77 K and RT (300 K) can be calculated to be 0.038 eV. This is in good agreement with the data of [E_c(77 K)-E_c (300 K)] in Table II, suggesting a tight connection between the E_g and E_c. Hence, the difference between E_g and E_c may be attributed to the existence of some band tail states, which are in a certain distance from the band edge.

TABLE II. Maximum responsivities ($R_{v,\max}$) and cutoff photon energies (E_c) obtained from the responsivity spectra of the photoconductors.

	$R_{v,\max}$ (V/W)		E_c (eV)		
Sample	77 K	300 K	77 K	300 K	E_c(77 K)−E_c(300 K) (eV)
A	30.4	0.15	0.150	0.113	0.037
C	28.3	0.26	0.136	0.098	0.038

In summary, we have grown high-quality $InAs_xSb_{1-x}$ films on GaAs substrates by LPE and fabricated photoconductors. The $InAs_xSb_{1-x}$ films exhibit Hall mobilities higher than 2×10^4 cm^2 V^{-1} s^{-1} and cutoff wavelengths longer than 10 μm at RT, implying that there are a low inside-grain dislocation density and structural ordering in the $InAs_xSb_{1-x}$ films. A notable photoresponse beyond 8 μm was observed with the photoconductors at RT. In particular, for the $InAs_xSb_{1-x}$ film with a midrange composition of $x=0.3$, the E_c is as low as 0.098 eV and there is a photoresponse of up to 13 μm with a maximum responsivity of 0.26 V/W at RT. Hence, LPE-grown $InAs_xSb_{1-x}/GaAs$ has demonstrated attractive properties for use in RT long-wavelength infrared detectors.

The authors would like to thank Yanli Ji for the detector fabrication. This work was supported by the National Natural Science Foundation of China (Grant No. 60576010) and the Special Funds for Major State Basic Research Projects of China (Grant No. 2002CB311905).

[1] S.-H. Wei and A. Zunger, Appl. Phys. Lett. **58**, 2684 (1991).
[2] G. P. Srivastava, J. L. Martins, and A. Zunger, Phys. Rev. B **31**, 2561 (1985).
[3] H. R. Jen, K. Y. Ma, and G. B. Stringfellow, Appl. Phys. Lett. **54**, 1154 (1989).
[4] S. R. Kurtz, L. R. Dawson, R. M. Biefeld, D. M. Follstaedt, and B. L. Doyle, Phys. Rev. B **46**, 1909 (1992).
[5] J.-l. Chyi, S. Kalem, N. S. Kumar, C. W. Litton, and H. Morkoc, Appl. Phys. Lett. **53**, 1092 (1988).
[6] C. G. Bethea, M. Y. Yen, B. F. Levine, K. K. Choi, and A. Y. Cho, Appl. Phys. Lett. **51**, 1431 (1987).
[7] M. Y. Yen, R. People, and K. W. Wecht, J. Appl. Phys. **64**, 952 (1988).
[8] M. Y. Yen, J. Appl. Phys. **64**, 3306 (1988).
[9] C. G. Bethea, B. F. Levine, M. Y. Yen, and A. Y. Cho, Appl. Phys. Lett. **53**, 291 (1988).
[10] R. M. Biefeld, J. Cryst. Growth **75**, 255 (1986).
[11] K. T. Huang, Y. Hsu, R. M. Cohen, and G. B. Stringfellow, J. Cryst. Growth **156**, 311 (1995).
[12] C. Besikci, Y. H. Choi, G. Labeyrie, E. Bigan, M. Razeghi, J. B. Cohen, J. Carsello, and V. P. Dravid, J. Appl. Phys. **76**, 5820 (1994).
[13] J. D. Kim, S. Kim, D. Wu, J. Wojkowski, J. Xu, J. Piotrowski, E. Bigan, and M. Razeghi, Appl. Phys. Lett. **67**, 2645 (1995).
[14] J. D. Kim, D. Wu, J. Wojkowski, J. Piotrowski, J. Xu, and M. Razeghi, Appl. Phys. Lett. **68**, 99 (1996).
[15] A. S. Popov, A. M. Koinova, and S. L. Tzeneva, J. Cryst. Growth **186**, 338 (1998).
[16] V. K. Dixit, B. Bansal, V. Venkataraman, H. L. Bhat, K. S. Chandrasekharan, and B. M. Arora, J. Appl. Phys. **96**, 4989 (2004).
[17] R. J. Egan, V. M. L. Chin, and T. L. Tansiey, J. Appl. Phys. **75**, 2473 (1994).
[18] J. C. Woolley and J. Warner, Can. J. Phys. **42**, 1879 (1964).
[19] See, e. g., S. Adachi, *Physical Properties of III-V Semiconductor Compounds* (Wiley, New York, 1992), p. 275.
[20] Y. P. Varshni, Physica (Utrecht) **34**, 149 (1967).